

AdapNet: Adaptive Noise-Based Network for Low-Quality Image Retrieval

Sihe Zhang^{1*} Qingdong He^{2*} Jinlong Peng^{2*} Yuxi Li² Zhengkai Jiang²
 Jiafu Wu² Mingmin Chi¹ Yabiao Wang² Chengjie Wang²
¹Fudan University ²Youtu Lab, Tencent

Abstract

Image retrieval aims to identify visually similar images within a database using a given query image. Traditional methods typically employ both global and local features extracted from images for matching, and may also apply re-ranking techniques to enhance accuracy. However, these methods often fail to account for the noise present in query images, which can stem from natural or human-induced factors, thereby negatively impacting retrieval performance. To mitigate this issue, we introduce a novel setting for low-quality image retrieval, and propose an Adaptive Noise-Based Network (AdapNet) to learn robust abstract representations. Specifically, we devise a quality compensation block trained to compensate for various low-quality factors in input images. Besides, we introduce an innovative adaptive noise-based loss function, which dynamically adjusts its focus on the gradient in accordance with image quality, thereby augmenting the learning of unknown noisy samples during training and enhancing intra-class compactness. To assess the performance, we construct two datasets with low-quality queries, which is built by applying various types of noise on clean query images on the standard Revisited Oxford and Revisited Paris datasets. Comprehensive experimental results illustrate that AdapNet surpasses state-of-the-art methods on the Noise Revisited Oxford and Noise Revisited Paris benchmarks, while maintaining competitive performance on high-quality datasets. The code and constructed datasets will be made available.

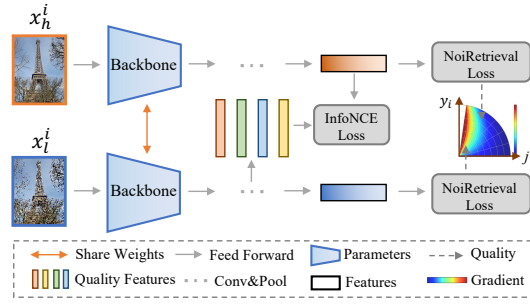
1 Introduction

The objective of instance-level image retrieval is to search for and retrieve images from a large scale dataset containing the same object as depicted in a given query image. Over the past two decades, various handcrafted feature-based methods [19, 37] have been proposed to enhance the performance of instance level image retrieval. Recently, with advancements in deep learning technologies, deep feature representations have emerged as the dominant approach [22]. The development of deep neural networks enables the extraction of high-level features that capture complex patterns and semantics, leading to improved retrieval performance [1, 2, 28].

However, the efficiency of image retrieval can be severely affected by the quality of query, which is influenced by factors such as resolution, lighting, noise, and compression artifacts [17]. A straightforward solution is to include a portion of the noisy dataset as part of the training dataset, but this potentially leads reliance on less reliable visual cues, such as color or textures, to compensate for lost identity information, resulting in inaccurate results [9]. This problem can also be partially addressed through the use of diverse techniques, including denoising, super-resolution, and image enhancement, which belong to low level improvements at the image level [21]. Recent studies start to focus on the training process and aim to guide the model to learn

*Equal contributions.

robust representation across different image qualities while keeping the discrimination ability. AdaFace [12] typically proposes a new adaptive margin loss function that emphasizes samples of varying difficulties based on their image qualities. These studies have demonstrated some improvements in recognition accuracy [31]. Nevertheless, AdaFace is trained by sacrificing certain noise data, which may result in relatively weaker discriminative representation.



With the consideration above, in this paper, we propose a novel setting for low-quality image retrieval to retrieve normal images from a database when given low-quality queries. To achieve this, we construct two new noisy datasets by adding various types of random noise to the original test datasets, Revisited Oxford and Revisited Paris [24]. The noisy dataset is specifically designed to simulate both natural or artificial factors degrading image quality. Judging from partial experimental results, conventional methods struggles in our new benchmarks, making it necessary to develop more robust and adaptive models to handle the disparity in image quality. To address this new problem, we aim to design a noise-based network, as shown in Figure 1, to learn robust abstract representations in low quality images. Specifically, we propose a quality compensation block that leverages high-quality reference images to facilitate the model’s understanding of various known noise characteristics. Furthermore, we introduce a novel adaptive noise-based loss function, NoiRetrieval Loss, that dynamically adjusts its attention to gradients based on the quality of images. This adaptive mechanism allows model to enhance unknown noise learning during training and promote intra-class compactness. Our main contributions are summarized as follows:

Figure 1: Overview of our proposed method. The current high-quality image input x_h^i and low-quality image input x_l^i are fed into the backbone to generate corresponding embeddings. Quality compensation features in multiple colors are employed to learn known noise, and NoiRetrieval Loss is utilized to dynamically adjust the gradient of unknown noise according to image quality.

- We introduce a novel setting for low-quality image retrieval and propose an adaptive noise-based network (AdapNet) to learn robust abstract representations in low-quality images.
- We design a quality compensation block that utilizes high-quality reference images to enhance model’s comprehension of different known noise characteristics.
- To enhance the model’s denoising capability against unknown noise, we design a noise-based loss named NoiRetrieval Loss, which pays more attention to the learning of low-quality samples.
- Through extensive experiments, the proposed method achieves stage-of-the-art low-quality image retrieval performance on our new benchmarks: Noise ROxf (+1M), Noise RPar (+1M) while maintaining competitive performance on the original high-quality datasets.

2 Related Work

2.1 Image Retrieval

In earlier studies, techniques such as Fisher vector [11], VLAD [10], or ASMK [27] were used to develop global features by aggregating hand-crafted local features. Subsequently, spatial verification methods, such as RANSAC [6], were employed to refine the initial retrieval results by performing local feature matching. Recently, handcrafted features have been replaced by global and local features extracted from deep learning networks. Notable advancements have been made by leveraging discriminative geometry information in studies [36, 8, 4, 29]. CVNet [14] use curriculum learning with the hard negative mining and Hide-and-Seek strategy to handle hard samples without losing generality. The state-of-the-art approach CFCD [38] attentively selects prominent local descriptors and infuses fine-grained semantic relations into the global representation. SENet [13] captures the internal structure of the images and gradually compresses them into dense self-similarity descriptors while learning diverse structures from various images. Despite the varying quality of images in the dataset, these approaches overlook the impact of noise on image retrieval performance. Consequently,

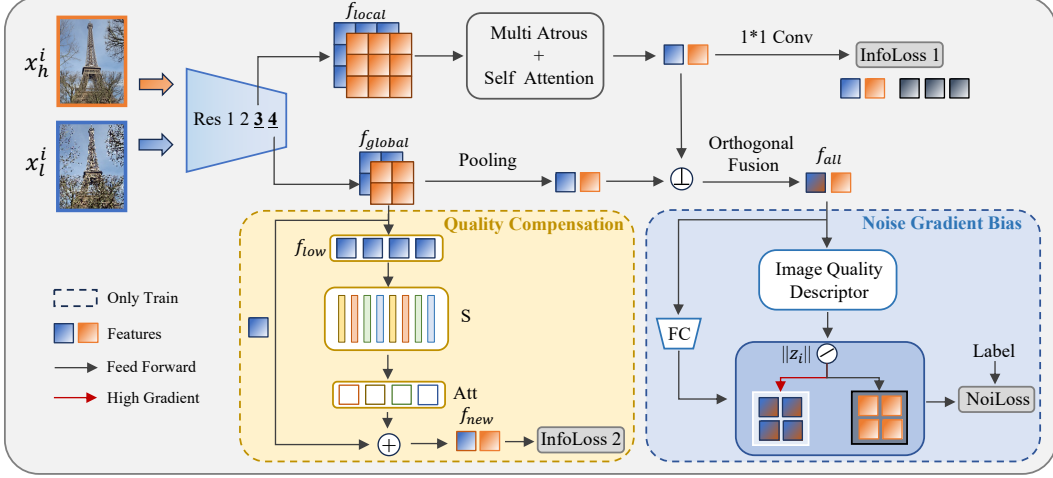


Figure 2: The detail structure of our proposed Adaptive Noise-Based Network (AdapNet). Our network is organized into three components: Backbone, Quality Compensation Block (QCB), and Noise Gradient Bias (NGB). The Backbone extracts the local embedding f_{local} and global embedding f_{global} of input images. The QCB learns the compensation features from the extracted global features of the input image pairs and integrates them with the low-quality features to form f_{new} . The NGB adjusts the allocation of gradients to the final features f_{all} based on image quality $\|z_i\|$, prioritizing the learning of low-quality images.

the inclusion of low-quality query images can significantly reduce the overall retrieval effectiveness [35]. Taking this into consideration, we introduce a training approach that uses pairs of high and low-quality images, deliberately introduces noise, and proposes a quality compensation block to improve the model’s understanding of various known noise characteristics.

2.2 Recognition with Low-Quality Images

Currently, the work on low-quality image recognition or retrieval is particularly prevalent in the field of face recognition, primarily due to the availability of naturally noisy datasets. Optimal performance depends on two key aspects: 1) mastering the extraction of discriminative features from low-quality images, and 2) developing the ability to discard images that contain few identity cues, a process often termed as quality-aware fusion [12]. To improve quality-aware fusion, many studies have achieved high performance to predict uncertainty representation [3, 16, 25]. While AdaFace [12] has shown effectiveness in face recognition tasks by incorporating image quality to dynamically update the model’s gradient weights. It is designed to disregard those low-quality images that are difficult to recognize rather than emphasize learning from low-quality images. Face recognition primarily focuses on identifying or verifying the identity of individuals in images or videos. It grapples with challenges such as variations in facial expressions, poses and other natural noises [15]. The image retrieval task also faces similar noise issues as the face recognition task. Therefore, we design a noise-based loss named NoiRetrieval Loss, which pays more attention to the learning of low-quality samples and introduce a new setting for low-quality image retrieval, aiming to locate visually similar images to a given query within a database, even when the query images are of poor qualities.

3 Methods

3.1 Problem Setup and Overview

Recent researches focus on the essential details of an image, thereby enabling efficient image matching. However, the presence of noise, which can originate from natural elements or device-related factors, is often inconsistent across different datasets. This noise can significantly influence the model’s image retrieval capabilities [20]. With this challenge in mind, we restructure the conventional image retrieval training input, which typically consists of pairs of low and high-quality images. These paired images are then fed into the network concurrently. Subsequently, we propose a Quality Compensation Block to learn the features associated with the artificially induced noise in the image samples. By emphasizing these noise-specific features, model can effectively differentiate noise from specific

image content. In addition to the artificially induced noise, we introduce a Noise Gradient Bias to prioritize the learning of general noise patterns present in low-quality images, enabling the model to handle various types and degrees of unknown noise.

The training datasets include high-quality dataset $\{X_{high}\}$ and low-quality dataset $\{X_{low}\}$. Then inputs are N image pairs $\{x_h^i, x_l^i : i \in [1, N], x_h^i \in X_{high}, x_l^i \in X_{low}\}$. We use $f_{local}, f_{global} \in \mathbb{R}^{C \times H \times W}$ as the feature map (channels C , height H , width W) of the input images. f_{global} serves as the input for Quality Compensation Block \mathcal{S} , f_{local} is used to extract local features, and ultimately they are fused into $f_{all} \in \mathbb{R}^{C^* \times 1 \times 1}$ (channels C^*), which is then inputted into the Noise Gradient Bias for Image Quality Descriptor z extraction and classification.

3.2 Quality Compensation Block

Since an image pair comes from the same image, the local features are nearly identical. This module aims to learn feature compensation from low-quality to high-quality images through input image pairs. Due to the strong robustness of InfoNCE loss [23], this compensation is reflected in abstract features. The specific network architecture is depicted in Figure 2. Quality Compensation Block includes eight convolution kernels, used to extract eight different types of noise from the low-quality images. Given the uncertainty of the specific type of noise present in the input image, which could even contain multiple noise types, we selectively fuse multiple compensation features using a 1×1 convolution layer and an adaptiveavgpool2d pooling layer. This fusion process allows the model to adapt to various noise combinations effectively. The entire processing flow of the module can be simplified as follows:

$$f_{new} = \sum_{i=1}^N (Att(\mathcal{S}_i(f_{low}))) + f_{low} \quad (1)$$

where \mathcal{S}_i is employed to represent N different compensation operations and the term Att is used to denote the integration of all compensation features. In Figure 2, the variable f_{global} consists of two components: f_{low} and f_{high} , representing the image features of low-quality and high-quality images, respectively. To clarify, we select f_{low} as the input for the quality compensation block. The learned compensation features and the original low-quality features are then added together at the element-wise level to obtain new features f_{new} , which are used to combined with the corresponding high-quality image features to compute the InfoNCE loss.

$$\mathcal{L}_{info} = -\frac{1}{N} \sum_{i=1}^N \log \left(\frac{\exp(\cos(f_{new}^i, f_{high}^i))}{\sum_{j=1}^N \exp(\cos(f_{new}^i, f_{high}^j))} \right) \quad (2)$$

where N signifies the number of low-quality samples. f_{new}^i and f_{high}^i correspondingly denote the feature vectors of the i th sample and the positive sample. \cos represents the similarity function.

3.3 Noise Gradient Bias

The cross entropy softmax loss of a sample x_i can be formulated as follows,

$$l_{CE}(x_i) = -\log \frac{\exp(W_{y_i} z_i + b_i)}{\sum_{j=1}^C \exp(W_j z_j + b_j)} \quad (3)$$

where $z_i \in \mathbb{R}^d$ is the feature embedding of x_i , and x_i belongs to the y_i th class. W_j refers to the j th column of the last FC layer weight matrix, $W \in \mathbb{R}^{d \times C}$, and b_j refers to the corresponding bias term. C refers to the number of classes. To directly optimize the cosine distance in the training objective, [18] use normalized softmax during training. The transformed formula is as follows

$$l_{CE}(x_i) = -\log \frac{\exp(s \cdot \cos \theta_{y_i})}{\sum_{j=1}^C \exp(s \cdot \cos \theta_j)} \quad (4)$$

where θ_j corresponds to the angle between z_i and W_j , s denotes a scale value. In the molecular terms, the component $\exp(s \cdot \cos \theta_{y_i})$ is commonly defined as $f(\theta_{y_i}, m)$ to enable flexible handling of features across different categories. Based on this, we design a novel loss function based on image quality different from AdaFace [12] as follows.

3.3.1 Image Quality Descriptor

Image quality encompasses various characteristics, including brightness, contrast, motion blur and so on. In the recent AdaFace work, researchers employ the feature norm as a proxy for image quality. It is observed that models trained with a margin-based softmax loss exhibit a correlation between the feature norm and image quality, indicating a obvious trend. Building upon the quality discrimination method used in AdaFace, we make specific modifications to adapt it to a new loss function called NoiRetrieval Loss. The modified Image Quality Descriptor can be formulated as follows:

$$\widetilde{\|z_i\|} = \frac{1}{2} \left[\left[\frac{\|z_i\| - \mu_z}{\sigma_z/h} \right]_{-1}^1 + 1 \right] \quad (5)$$

where $\|z_i\|$ is the feature norm, μ_z and σ_z are the mean and standard deviation of all $\|z_i\|$ within a batch. We introduce the term h to control the concentration and linearly map the original distribution interval from $[-1, 1]$ to $[0, 1]$ to ensure monotonicity of $\cos z$ in this range.

3.3.2 NoiRetrieval Loss

To prioritize the learning of unknown noise patterns typically observed in low-quality images, we design a noise-based loss function according to Image Quality Descriptor. This function emphasizes learning from these images, regardless of whether they are easily recognizable samples or more challenging ones. Specifically,

$$f(\theta_j, \widetilde{\|z_i\|})_{Noi} = \begin{cases} s[\cos \widetilde{\|z_i\|} * \cos(\theta_j + m)] & j = y_i \\ s \cos \theta_j & j \neq y_i \end{cases} \quad (6)$$

where we can observe that when the quality of the image is higher, the value of $\widetilde{\|z_i\|}$ is larger, which in turn reduce the value of $f(\theta_j, \widetilde{\|z_i\|})_{Noi}$. This implies that model needs to decrease θ_j to restore the value of $f(\theta_j, \widetilde{\|z_i\|})_{Noi}$ to its original size, indicating a more strict feature classification for high-quality images. This does not mean the model overlooks low-quality images. On the contrary, during the backpropagation process, it is often the case that gradients from low-quality images are assigned higher weights, rather than at the numerical level when calculating the loss. Let $P_j^{(i)}$ be the probability output at class j after the softmax operation on an input x_i . By deriving the gradient equations for L_{CE} w.r.t W_j and x_i , we obtain the following,

$$P_j^{(i)} = \frac{\exp(f(\cos \theta_{y_i}))}{\exp(f(\cos \theta_{y_i})) + \sum_{j \neq y_i} \exp(s \cos \theta_j)} \quad (7)$$

we can denote a gradient scaling term (GST) [12] as

$$g := (P_j^{(i)} - \mathbb{1}(y_i = j)) \frac{\partial f(\cos \theta_j)}{\partial \cos \theta_j} \quad (8)$$

since in our model $f(\cos \theta_{y_i}) = s[\cos \widetilde{\|z_i\|} * \cos(\theta_j + m)]$ and $\frac{\partial f(\cos \theta_{y_i})}{\partial \cos \theta_{y_i}} = s$, the gradient of NoiRetrieval Loss is

$$g_{Noi} = (P_j^i - 1) \cos \widetilde{\|z_i\|} \left(\cos(m) + \frac{\cos \theta_{y_i} \sin(m)}{\sqrt{1 - \cos^2 \theta_{y_i}}} \right) s \quad (9)$$

To better illustrate the gradient function, we opt to visually represent it using a heatmap, as shown in Figure 3. In this heatmap, we compare the gradients from different dimensions and observe

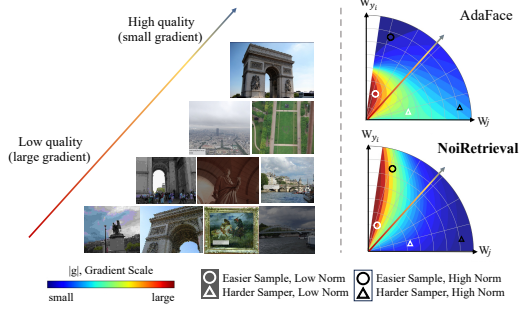


Figure 3: Here we illustrate NoiRetrieval Loss, AdaFace Loss, and their corresponding gradient scaling terms within the feature space. The arc in the feature space represents the angular relationship between a sample and the ground truth class weight vector, W_{y_i} , as well as the negative class weight vector W_j . A well-classified sample will be proximate, in terms of angle, to the ground truth class weight vector, W_{y_i} . Conversely, a misclassified sample will be closer to W_j . The color within the arc represents the magnitude of the gradient scaling term g . Samples located in the dark red region will contribute more significantly to the learning process.

that as the radius increases, which implies a higher quality, the gradient value decreases in both AdaFace [12] and NoiRetrieval to make the model focus on learning from lower quality images. Moreover, NoiRetrieval tends to allocate more gradients towards simpler samples across different qualities, thereby preserving more sample information, instead of focusing solely on challenging samples as AdaFace [12] does when image quality is relatively higher.

Based on the proposed NoiRetrieval Gradient Bias module, we design a novel loss function \mathcal{L}_{Noi} which is defined as:

$$\mathcal{L}_{Noi} = -\frac{1}{N} \sum_{i=1}^N \log \frac{e^{s[\cos\|z_{y_i}\|(\cos(\theta+m))]} }{e^{s[\cos\|z_{y_i}\|(\cos(\theta+m))]} + B} \quad (10)$$

where y_i is the ground-truth label, m is a margin value, the specific value of which will be provided in the experimental section. θ represents the angle between the computed feature vector and corresponding label vectors in the mini-batch with size N . $B = \sum_{j \neq y_i}^n e^{s \cos \theta_j}$ is used to calculate the cosine similarity between the current feature vector and other class vectors.

3.4 Training Objective

We incorporate the InfoNCE loss into two components of the network, as depicted in the network architecture diagram. \mathcal{L}_{Info1} is employed to ensure the similarity between low-quality and high-quality local features, while \mathcal{L}_{Info2} supervises the learning of distinct compensation features. Regarding \mathcal{L}_{Noi} , it serves to oversee the feature vector that the entire model outputs. Once mapped into the feature space, it assesses the similarity with each category and dynamically adjusts the gradient weights according to the image quality. Hence, it is a primary target for optimization during model training. The final loss function of our proposed network is:

$$\mathcal{L}_{All} = \mathcal{L}_{Noi} + \alpha \mathcal{L}_{Info1} + \beta \mathcal{L}_{Info2} \quad (11)$$

where α and β are two weights to fuse.

4 Experiments

4.1 Implementation Details

4.1.1 Dataset and Evaluation Metric

We utilize the GLDv2-clean subset of the Google Landmarks dataset v2 [30] (referred to as GLDv2-clean) as our training dataset. GLDv2-clean comprises 1,580,470 images from 81,313 landmarks, encompassing a wide range of different landmarks. Based on this dataset, we create a new noisy dataset, GLDv2-noisy, by randomly adding various types of noise to the entire dataset using eight manually defined noise functions. During model training, the input images consist of half of the original dataset, while the other half is comprised of the generated noisy dataset. For the evaluation of our model, we utilize the ROxford5k and RParis6k datasets, referred to as ROxf and RPar, respectively. These datasets consist of 70 queries and include 4993 and 6322 database images, respectively. Additionally, we employ the R1M dataset [24], which contains one million distractor images, to measure the performance of large-scale retrieval. In order to ensure robustness and evaluate the performance of our model under noisy conditions, we introduce random noise to the original datasets, resulting in the Noise ROxford5k and Noise RParis6k datasets, similar to the training dataset. To ensure a fair comparison, we use the mean average precision (mAP) as our evaluation metric on both datasets, following the Easy, Medium and Hard difficulty protocols. Besides, we define another evaluation metric called Noise mAP when query images come from the noisy dataset.

4.1.2 Training details

ResNet50 and ResNet101 [7] are employed as the backbone for conducting experiments in this study. Prior to training, the images are resized to dimensions of 512×512 , following the methodology established in previous works [33, 14]. The training process is performed on 8 V100 GPUs for 100 epochs utilizing a batch size of 256. We use the SGD optimizer with a momentum of 0.9. A weight decay factor of 0.0001 is applied, and we adopt the cosine learning rate decay strategy. For the NoiRetrieval Loss, we empirically set the margin parameter m to 0.15. As for global feature

Table 1: Result comparisons with baselines on Low-Quality Image Retrieval(% mAP)

Method	Easy				Medium				Hard			
	Roxf	+1M	Rpar	+1M	Roxf	+1M	Rpar	+1M	Roxf	+1M	Rpar	+1M
<i>Clear to Clear</i>												
AdaFace [12]	87.2	77.1	91.5	83.8	65.5	54.1	79.9	63.5	35.1	22.3	60.7	36.8
CVNet [14]	81.5	68.2	92.4	80.2	59.1	44.7	80.3	56.9	28.2	15.8	60.3	27.8
CFCD [38]	82.3	68.6	93.2	82.7	60.1	45.8	80.6	60.0	26.2	14.9	61.6	30.7
SENet [13]	77.6	61.1	91.0	76.3	55.1	39.5	78.5	52.4	21.6	10.2	57.9	22.3
AdapNet(Ours)	87.5	77.3	94.3	87.3	67.1	54.5	85.0	67.8	37.7	24.1	69.4	40.8
<i>Noise to Clear</i>												
AdaFace [12]	71.8	58.6	81.4	66.4	53.1	38.9	69.6	48.6	25.4	11.6	49.6	26.2
CVNet [14]	72.1	53.5	86.1	65.4	50.9	34.0	73.3	44.9	21.3	9.0	51.2	20.8
CFCD [38]	70.2	48.9	80.1	63.0	49.5	30.8	69.4	44.7	18.8	8.0	48.9	21.4
SENet [13]	64.5	44.4	82.5	61.9	46.2	28.0	70.9	42.0	17.6	6.2	48.9	16.6
AdapNet(Ours)	75.4	60.4	86.2	69.1	57.1	41.1	76.3	52.1	30.2	14.4	58.2	29.7

extraction, we produce multi-scale representations as well, using 5 scales, $\left\{\frac{1}{2\sqrt{2}}, \frac{1}{2}, \frac{1}{\sqrt{2}}, 1, \sqrt{2}\right\}$, to extract final compact feature vectors. Following previous works [22, 2]. For each scale independently, an L2 normalization is applied. These normalized features are then average-pooled to produce the final descriptor [5]. We use two kinds of experimental settings to ensure fair comparisons.

4.2 Experimental Results

In Table 1, results (% mAP) of different solutions are obtained following the Easy, Medium and Hard evaluation protocols of Roxf (+1M), Rpar (+1M) and their noisy dataset. The methods mentioned in Table 1 all use one-tenth of the dataset from “GLDv2-clean” and “GLDv2-noisy” as the training dataset. “Clear to Clear” represents a scenario where both the query image and the image to be retrieved are of high-quality. Conversely, “Noise to Clear” means the query image is a noisy image, while the image to be retrieved is of high-quality. ResNet50 is uniformly utilized for models that necessitate the use of the ResNet architecture, and pre-trained weights are imported. It can be observed that our solution consistently outperforms existing methods.

4.2.1 Comparison with the state-of-the-art models

We re-implement CVNet [14], CFCD [38] and SENet [13] in the official configuration. Notably, our method outperforms the CFCD with a gain of up to 6.9% on Rpar-Medium, 9.3% on Rpar-Hard in the “Noise to Clear” setting and 4.4% on Rpar-Medium, 7.8% on Rpar-Hard in the “Clear to Clear” setting. Even with the addition of another one million images to the database, AdapNet still outperform CFCD by a large margin, respectively, which demonstrates the effectiveness of our method to robust image retrieval. When compared with CVNet and SENet, the proposed AdapNet exhibits significantly superior performance across both datasets. These results exhibit excellent performance of our framework for low-quality image retrieval.

For fairness, we compare our proposed model with the state-of-the-art image retrieval models over the years under the original settings in Table 2. We utilized 80% of the “GLDv2-clean” dataset for training, employing ResNet50 and ResNet101 as the foundational architectures. Results (% mAP) of different solutions are obtained following the Medium and Hard evaluation protocols of Roxf and Rpar. “*” indicates that “GLDv2-clean” is used and “◇” indicates that “SfM-120k” is used as the training dataset. State-of-the-art performances are marked in bold and our results are summarized at the bottom. The underlined numbers represent the best performances. After a training period of 100 epochs, we conducted tests on Roxf and Rpar, as detailed in Table 2. As can be seen, although our model focus on noisy images learning, it still performs well in traditional image retrieval tasks.

4.2.2 Comparison with the face recognition models

Since AdaFace [12] method is designed to train better in the presence of unidentifiable images in the training data, we incorporate it into our model for comparison. As can be seen in Table 1, AdaFace has a slight advantage over traditional image retrieval methods in scenario “Noise to Clear”, but there is still a significant gap compared to our model. Specifically, our method outperforms the AdaFace

Table 2: Result comparisons with baselines on Image Retrieval(% mAP)

Method	Medium				Hard			
	Roxf	+IM	Rpar	+IM	Roxf	+IM	Rpar	+IM
<i>(A) Local feature aggregation</i>								
R101-HOW-VLAD* [10]	73.5	60.4	82.3	62.6	51.9	33.2	67.0	41.8
R101-HOW-ASMK* [27]	80.4	70.2	85.4	68.8	62.5	45.4	70.8	45.4
R50-FIRE-ASMK \diamond [27]	81.8	66.5	85.3	67.6	61.2	40.1	70.0	42.9
R50-MDA-ASMK \diamond [27]	81.8	68.7	83.3	64.7	62.2	45.3	66.2	38.9
R50-Token* [31]	80.5	68.3	87.6	73.9	62.1	43.4	73.8	53.3
R101-Token* [31]	82.3	70.5	89.3	76.7	66.6	47.3	78.6	55.9
<i>(B) Global single-pass</i>								
R101-GeM+DSM \diamond [2]	65.3	47.6	77.4	52.8	39.2	23.2	56.2	25.0
R50-DELG* [26]	78.3	67.2	85.7	69.6	57.9	43.6	71.0	45.7
R101-DELG* [26]	81.2	69.1	87.2	71.5	64.0	47.5	72.8	48.7
R50-DOLG* [32]	80.0	70.5	89.5	77.9	60.8	44.6	77.5	57.5
R101-DOLG* [32]	82.0	72.4	90.1	80.2	63.8	48.3	78.2	61.3
R50-CVNet-Global [14]l*	81.0	72.6	88.8	79.0	62.1	50.2	76.5	60.2
R101-CVNet-Global [14]l*	80.2	74.0	90.3	80.6	63.1	53.7	79.1	62.2
R50-CFCD* [38]	82.4	73.1	91.6	81.6	65.1	50.8	81.7	62.8
R101-CFCD* [38]	85.2	74.0	91.6	82.8	70.0	52.8	81.8	65.8
R50-SENet* [13]	81.9	74.2	90.0	79.1	63.0	52.0	78.1	59.9
R101-SENet* [13]	82.8	76.1	91.7	83.6	66.0	55.7	82.8	67.8
R50-SpCa* [34]	81.6	73.2	88.6	78.2	61.2	48.8	76.2	60.9
R101-SpCa* [34]	83.2	77.8	90.6	79.5	65.9	53.3	80.0	65.0
<i>Ours</i>								
R50-AdapNet*	81.4	71.3	88.2	78.9	63.9	48.7	74.5	59.2
R101-AdapNet*	82.2	72.8	90.5	81.9	64.6	51.1	79.6	64.7

with a gain of up to 6.7% on Rpar-Medium, 8.6% on Rpar-Hard in the “Noise to Clear” setting and 5.1% on Rpar-Medium, 8.7% on Rpar-Hard in the “Clear to Clear” setting.

4.3 Ablation Studies

In this section, we conduct a series of ablation experiments using the ResNet50 backbone to empirically validate the components of AdapNet. The methods mentioned in Table 3 use one-tenth of the dataset from “GLDv2-clean” and “GLDv2-noisy” as the training dataset.

Table 3: Results (% mAP & Noise mAP) of ablation experiments on different modules.

Method	InfoLoss 1	Quality Compensation	mAP			Noise mAP		
			Easy	Medium	Hard	Easy	Medium	Hard
AdaFace (baseline)	×	None	91.5	79.9	60.7	81.4	69.6	49.6
AdaFace*	×	None	92.6	81.3	63.4	86.2	74.1	53.8
NoiRetrieval	×	None	94.0	84.2	67.8	85.4	75.3	56.5
	✓	None	94.0	84.4	68.4	86.1	76.2	57.7
	×	CrossEntropy	93.9	83.7	66.1	79.5	69.5	51.3
	×	InfoLoss 2	94.0	83.9	67.5	86.1	75.5	57.4
	✓	InfoLoss 2	94.3	84.9	69.4	86.2	76.3	58.2

4.3.1 Effect of the proposed modules

Ablation studies are conducted on the proposed modules to demonstrate their effectiveness. Starting with AdaFace as the baseline, we experiment with various modifications. Initially, we only adjust the Image Quality Descriptor, resulting in the creation of the AdaFace* method, which employs the same image quality descriptor as ours. As demonstrated in Table 3, this adjustment leads to an approximate 4% improvement over the baseline in Noise mAP. Based on this, we design the NoiRetrieval Loss, which yields significant improvement in both low-quality and conventional image retrieval, notably achieving an approximate 7% increase in the Hard category. In subsequent experiments, the NoiRetrieval foundation is augmented with additional modules. CrossEntropy Loss is initially employed in the quality compensation block, but this results in a performance decline. Considering the abstract nature of compensation features, the blurred distinctions between various noise, and the occurrence of multiple noise types within a single image, we choose to employ the more resilient InfoNCE loss. After numerous adjustments and experiments, it is found that using InfoNCE loss to compute similarity loss enhances the model’s performance.

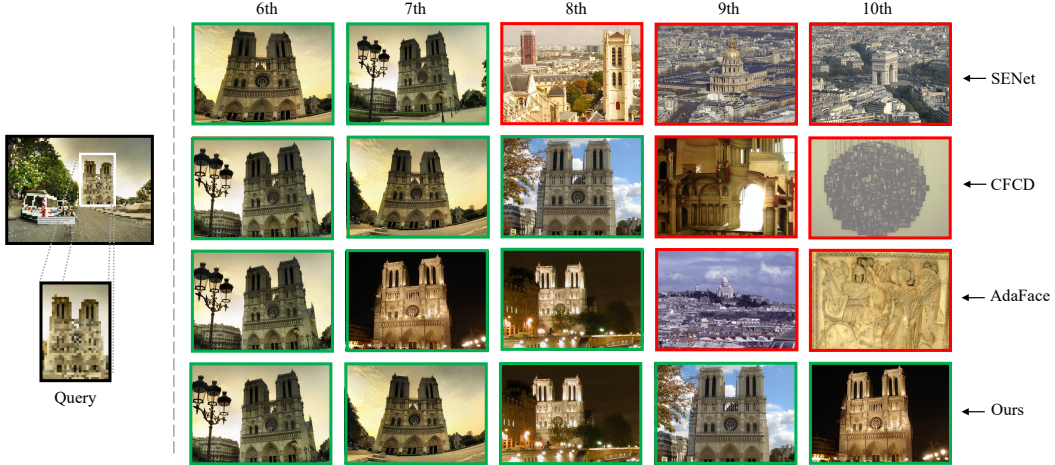


Figure 4: The demonstrations of the top retrieved results (ranks 6-10) are shown. The image on the left, used as a query image, is generated by cropping only the part bounded by a white box. On the right, we present the results of CFCD [38] and SENet [13] AdaFace [12], and our method, displayed from top to bottom. Images enclosed in green and red boxes denote positive and negative images, respectively.

After determining the basic design of the model, we attempt to optimize the model’s loss function \mathcal{L}_{All} , fixing the coefficient of \mathcal{L}_{Noi} at 1, while α and β serve as the hyperparameters. Based on this, we design the following set of experiments, as shown in Table 4. We find that the results are relatively satisfactory when α and β are both set to 0.2.

Table 4: Results (% mAP & Noise mAP) of ablation experiments on different α and β in \mathcal{L}_{Info} .

\mathcal{L}_{Noi}	\mathcal{L}_{Info}		mAP			Noise mAP		
	α	β	Easy	Medium	Hard	Easy	Medium	Hard
1	0.1	0.1	94.3	84.9	69.4	86.2	76.3	58.2
1	0.2	0.2	94.7	84.8	68.7	87.3	77.3	58.4
1	0.2	0.5	94.5	83.9	67.3	87.3	76.6	57.4
1	0.5	0.5	94.3	84.4	68.4	87.8	77.0	58.6

4.3.2 Qualitative results

Example qualitative results are shown in Figure 4. Despite advanced feature representation, previous solutions that do not consider the quality of images are easily fooled by noise in the dataset. Our proposed network captures known noise and strengthens the learning of unknown noise, thereby enhancing the model’s ability to resist noise interference. The retrieval results clearly demonstrate that our model surpasses the other methods when the query image is of low-quality.

5 Conclusion

In this work, we introduce a novel setting for low-quality image retrieval and develop an Adaptive Noise-Based Network (AdapNet) to learn robust abstract representations. Specifically, we incorporate a quality compensation block to eliminate known noise from images and devise an innovative adaptive noise-based loss function that dynamically focuses on the gradient relative to image quality, aiming to intensify the learning of unknown noise. Our comprehensive experiments show significant enhancements over state-of-the-art methods on low-quality datasets, while preserving competitive performance on high-quality datasets.

Limitations and Broader Impact. The model relies on the pre-training scheme and the structure of the quality compensation module can be designed more ingeniously. This study enhances image retrieval accuracy in noisy conditions, which can be beneficial for applications involving low-quality images. The proposed datasets and methodologies offer initial insights for future research in handling noisy data in image retrieval tasks.

References

- [1] Relja Arandjelovic, Petr Gronat, Akihiko Torii, Tomas Pajdla, and Josef Sivic. Netvlad: Cnn architecture for weakly supervised place recognition. In *Proceedings of the IEEE conference on computer vision and pattern recognition*, pages 5297–5307, 2016.
- [2] Bingyi Cao, Andre Araujo, and Jack Sim. Unifying deep local and global features for image search. In *Computer Vision–ECCV 2020: 16th European Conference, Glasgow, UK, August 23–28, 2020, Proceedings, Part XX 16*, pages 726–743. Springer, 2020.
- [3] Jie Chang, Zhonghao Lan, Changmao Cheng, and Yichen Wei. Data uncertainty learning in face recognition. In *Proceedings of the IEEE/CVF conference on computer vision and pattern recognition*, pages 5710–5719, 2020.
- [4] Mihai Dusmanu, Ignacio Rocco, Tomas Pajdla, Marc Pollefeys, Josef Sivic, Akihiko Torii, and Torsten Sattler. D2-net: A trainable cnn for joint detection and description of local features. *arXiv preprint arXiv:1905.03561*, 2019.
- [5] Ufuk Efe, Kutalmis Gokalp Ince, and Aydin Alatan. Dfm: A performance baseline for deep feature matching. In *Proceedings of the IEEE/CVF conference on computer vision and pattern recognition*, pages 4284–4293, 2021.
- [6] Martin A Fischler and Robert C Bolles. Random sample consensus: a paradigm for model fitting with applications to image analysis and automated cartography. *Communications of the ACM*, 24(6):381–395, 1981.
- [7] Kaiming He, Xiangyu Zhang, Shaoqing Ren, and Jian Sun. Deep residual learning for image recognition. In *Proceedings of the IEEE conference on computer vision and pattern recognition*, pages 770–778, 2016.
- [8] Kun He, Yan Lu, and Stan Sclaroff. Local descriptors optimized for average precision. In *Proceedings of the IEEE conference on computer vision and pattern recognition*, pages 596–605, 2018.
- [9] Yuge Huang, Pengcheng Shen, Ying Tai, Shaoxin Li, Xiaoming Liu, Jilin Li, Feiyue Huang, and Rongrong Ji. Improving face recognition from hard samples via distribution distillation loss. In *Computer Vision–ECCV 2020: 16th European Conference, Glasgow, UK, August 23–28, 2020, Proceedings, Part XXX 16*, pages 138–154. Springer, 2020.
- [10] Hervé Jégou, Matthijs Douze, Cordelia Schmid, and Patrick Pérez. Aggregating local descriptors into a compact image representation. In *2010 IEEE computer society conference on computer vision and pattern recognition*, pages 3304–3311. IEEE, 2010.
- [11] Hervé Jégou, Florent Perronnin, Matthijs Douze, Jorge Sánchez, Patrick Pérez, and Cordelia Schmid. Aggregating local image descriptors into compact codes. *IEEE transactions on pattern analysis and machine intelligence*, 34(9):1704–1716, 2011.
- [12] Minchul Kim, Anil K Jain, and Xiaoming Liu. Adaface: Quality adaptive margin for face recognition. In *Proceedings of the IEEE/CVF conference on computer vision and pattern recognition*, pages 18750–18759, 2022.
- [13] Seongwon Lee, Suhyeon Lee, Hongje Seong, and Euntai Kim. Revisiting self-similarity: Structural embedding for image retrieval. In *Proceedings of the IEEE/CVF Conference on Computer Vision and Pattern Recognition*, pages 23412–23421, 2023.
- [14] Seongwon Lee, Hongje Seong, Suhyeon Lee, and Euntai Kim. Correlation verification for image retrieval. In *Proceedings of the IEEE/CVF Conference on Computer Vision and Pattern Recognition*, pages 5374–5384, 2022.
- [15] Qiufu Li, Xi Jia, Jiancan Zhou, Linlin Shen, and Jinming Duan. Unitsface: Unified threshold integrated sample-to-sample loss for face recognition. *arXiv preprint arXiv:2311.02523*, 2023.
- [16] Shen Li, Jianqing Xu, Xiaqing Xu, Pengcheng Shen, Shaoxin Li, and Bryan Hooi. Spherical confidence learning for face recognition. In *Proceedings of the IEEE/CVF Conference on Computer Vision and Pattern Recognition*, pages 15629–15637, 2021.
- [17] Weisi Lin and C-C Jay Kuo. Perceptual visual quality metrics: A survey. *Journal of visual communication and image representation*, 22(4):297–312, 2011.

- [18] Weiyang Liu, Yandong Wen, Zhiding Yu, Ming Li, Bhiksha Raj, and Le Song. Sphreface: Deep hypersphere embedding for face recognition. In *Proceedings of the IEEE conference on computer vision and pattern recognition*, pages 212–220, 2017.
- [19] David G Lowe. Distinctive image features from scale-invariant keypoints. *International journal of computer vision*, 60:91–110, 2004.
- [20] Qiang Meng, Shichao Zhao, Zhida Huang, and Feng Zhou. Magface: A universal representation for face recognition and quality assessment. In *Proceedings of the IEEE/CVF conference on computer vision and pattern recognition*, pages 14225–14234, 2021.
- [21] Mourad Nachaoui, L Afraites, and Amine Laghrib. A regularization by denoising super-resolution method based on genetic algorithms. *Signal Processing: Image Communication*, 99:116505, 2021.
- [22] Hyeonwoo Noh, Andre Araujo, Jack Sim, Tobias Weyand, and Bohyung Han. Large-scale image retrieval with attentive deep local features. In *Proceedings of the IEEE international conference on computer vision*, pages 3456–3465, 2017.
- [23] Aaron van den Oord, Yazhe Li, and Oriol Vinyals. Representation learning with contrastive predictive coding. *arXiv preprint arXiv:1807.03748*, 2018.
- [24] Filip Radenović, Ahmet Iscen, Giorgos Tolias, Yannis Avrithis, and Ondřej Chum. Revisiting oxford and paris: Large-scale image retrieval benchmarking. In *Proceedings of the IEEE conference on computer vision and pattern recognition*, pages 5706–5715, 2018.
- [25] Yichun Shi and Anil K Jain. Probabilistic face embeddings. In *Proceedings of the IEEE/CVF International Conference on Computer Vision*, pages 6902–6911, 2019.
- [26] Oriane Siméoni, Yannis Avrithis, and Ondřej Chum. Local features and visual words emerge in activations. In *Proceedings of the IEEE/CVF Conference on Computer Vision and Pattern Recognition*, pages 11651–11660, 2019.
- [27] Giorgos Tolias, Yannis Avrithis, and Hervé Jégou. Image search with selective match kernels: aggregation across single and multiple images. *International Journal of Computer Vision*, 116:247–261, 2016.
- [28] Giorgos Tolias, Tomas Jeníček, and Ondřej Chum. Learning and aggregating deep local descriptors for instance-level recognition. In *Computer Vision—ECCV 2020: 16th European Conference, Glasgow, UK, August 23–28, 2020, Proceedings, Part I* 16, pages 460–477. Springer, 2020.
- [29] Philippe Weinzaepfel, Thomas Lucas, Diane Larlus, and Yannis Kalantidis. Learning super-features for image retrieval. *arXiv preprint arXiv:2201.13182*, 2022.
- [30] Tobias Weyand, Andre Araujo, Bingyi Cao, and Jack Sim. Google landmarks dataset v2-a large-scale benchmark for instance-level recognition and retrieval. In *Proceedings of the IEEE/CVF conference on computer vision and pattern recognition*, pages 2575–2584, 2020.
- [31] Hui Wu, Min Wang, Wengang Zhou, Yang Hu, and Houqiang Li. Learning token-based representation for image retrieval. In *Proceedings of the AAAI Conference on Artificial Intelligence*, volume 36, pages 2703–2711, 2022.
- [32] Min Yang, Dongliang He, Miao Fan, Baorong Shi, Xuetong Xue, Fu Li, Errui Ding, and Jizhou Huang. Dolg: Single-stage image retrieval with deep orthogonal fusion of local and global features. In *Proceedings of the IEEE/CVF International conference on Computer Vision*, pages 11772–11781, 2021.
- [33] Shuhei Yokoo, Kohei Ozaki, Edgar Simo-Serra, and Satoshi Iizuka. Two-stage discriminative re-ranking for large-scale landmark retrieval. In *Proceedings of the IEEE/CVF Conference on Computer Vision and Pattern Recognition Workshops*, pages 1012–1013, 2020.
- [34] Zhongyan Zhang, Lei Wang, Luping Zhou, and Piotr Koniusz. Learning spatial-context-aware global visual feature representation for instance image retrieval. In *Proceedings of the IEEE/CVF International Conference on Computer Vision*, pages 11250–11259, 2023.
- [35] Jingxiao Zheng, Ruichi Yu, Jun-Cheng Chen, Boyu Lu, Carlos D Castillo, and Rama Chellappa. Uncertainty modeling of contextual-connections between tracklets for unconstrained video-based face recognition. In *Proceedings of the IEEE/CVF International Conference on Computer Vision*, pages 703–712, 2019.

- [36] Liang Zheng, Yi Yang, and Qi Tian. Sift meets cnn: A decade survey of instance retrieval. *IEEE transactions on pattern analysis and machine intelligence*, 40(5):1224–1244, 2017.
- [37] Yan-Tao Zheng, Ming Zhao, Yang Song, Hartwig Adam, Ulrich Buddemeier, Alessandro Bissacco, Fernando Brucher, Tat-Seng Chua, and Hartmut Neven. Tour the world: building a web-scale landmark recognition engine. In *2009 IEEE Conference on Computer Vision and Pattern Recognition*, pages 1085–1092. IEEE, 2009.
- [38] Yunquan Zhu, Xinkai Gao, Bo Ke, Ruizhi Qiao, and Xing Sun. Coarse-to-fine: Learning compact discriminative representation for single-stage image retrieval. In *Proceedings of the IEEE/CVF International Conference on Computer Vision*, pages 11260–11269, 2023.